

# The first XMM-Newton observations of the Soft Gamma-ray Repeater SGR 1900+14 <sup>1</sup>

S. Mereghetti, P. Esposito<sup>2</sup>, A. Tiengo

*INAF - IASF Milano, via Bassini 15, I-20133 Milano, Italy*

S. Zane

*Mullard Space Science Laboratory, University College London,  
Holmbury St. Mary, Dorking Surrey, RH5 6NT, United Kingdom*

R. Turolla

*Università di Padova, Dipartimento di Fisica, via Marzolo 8, I-35131 Padova, Italy*

L. Stella, G.L. Israel

*INAF - Osservatorio Astronomico di Roma, via Frascati 33,  
I-00040 Monteporzio Catone, Italy*

D. Götz

*CEA Saclay, DSM/DAPNIA/Service d'astrophysique, F-91191 Gif-sur-Yvette, France*

M. Feroci

*INAF - IASF Roma, v. Fosso del Cavaliere 100, I-00133 Roma, Italy*

## ABSTRACT

A  $\sim 50$  ks XMM-Newton observation of SGR 1900+14 has been carried out in September 2005, after almost three years during which no bursts were detected from this soft gamma-ray repeater. The 0.8-10 keV spectrum was well fit by a power law plus blackbody model with photon index  $\Gamma=1.9\pm 0.1$ , temperature  $kT=0.47\pm 0.02$  keV and  $N_H = (2.12 \pm 0.08) \times 10^{22}$  cm<sup>-2</sup>, similar to previous observations of this source. The flux was  $\sim 5 \times 10^{-12}$  erg cm<sup>-2</sup> s<sup>-1</sup>, a factor 2 dimmer than the typical value and the smallest ever seen from SGR 1900+14.

---

<sup>2</sup>Università di Pavia, Dipartimento di Fisica Nucleare e Teorica and INFN-Pavia, via Bassi 6, I-27100 Pavia, Italy

The long term fading of the persistent emission has been interrupted by the recent burst reactivation of the source. A target of opportunity XMM-Newton observation performed in April 2006 showed a flux  $\sim 15\%$  higher. This variation was not accompanied by significant changes in the spectrum, pulsed fraction and light curve profile. We searched for emission and absorption lines in the spectra of the two observations, with negative results and setting tight upper limits of 50–200 eV ( $3\sigma$ ), depending on the assumed line energy and width, on the equivalent width of lines in the 1-9 keV range.

*Subject headings:* stars: individual (SGR 1900+14) – stars: neutron

## 1. Introduction

The few X-/gamma-ray sources known as Soft Gamma-ray Repeaters (SGRs) are generally believed to provide the most convincing evidence for the existence of magnetars, i.e. neutron stars with magnetic fields well above the quantum critical value  $B_c = \frac{m_e^2 c^3}{e\hbar} = 4.4 \times 10^{13}$  G (Duncan & Thompson 1992; Paczynski 1992).

The first sources of this class were discovered in the seventies as transient emitters of short (tens of ms) bursts of hard X-rays (Mazets et al. 1979; Cline et al. 1980; Laros et al. 1986). Only in more recent years it was possible to identify and study in detail their counterparts in the classical 1–10 keV X-ray band. This led to the discovery of periodic pulsations and secular spin-down in SGR 1806–20 (P=7.5 s, Kouveliotou et al. 1998) and SGR 1900+14 (P=5.2 s, Hurley et al. 1999; Kouveliotou et al. 1999) thus confirming the neutron star nature of this class of sources. Occasionally, SGRs emit very energetic giant flares, during which up to a few  $10^{46}$  ergs are released in a few tenths of a second. The extreme properties of these events, of which only three, each one for a different source, have been observed to date, are the main motivation for the magnetar interpretation (Thompson & Duncan 1995, 1996).

Among the four confirmed SGRs, SGR 1806–20 and SGR 1900+14 offer the best prospects for detailed spectral and timing studies in the soft X-ray band (E<10 keV). Both these sources, despite alternating periods of bursting activity with intervals of quiescence lasting months or years, remained at flux levels of the order of  $10^{-11}$  erg cm $^{-2}$  s $^{-1}$ . The other

---

<sup>1</sup>Based on observations obtained with XMM-Newton, an ESA science mission with instruments and contributions directly funded by ESA Member States and NASA.

Galactic soft repeater, SGR 1627–41, had a similar X-ray flux when it was discovered as a bursting source in 1998 (Woods et al. 1999b), but since then its luminosity decreased by a factor  $\sim 25$  and it is now a rather faint source (Mereghetti et al. 2006). SGR 0526–66 has a relatively high luminosity ( $\sim 2 \times 10^{35}$  erg s $^{-1}$ ), but being at the Large Magellanic Cloud distance, its observed flux is only  $\sim 10^{-12}$  erg cm $^{-2}$  s $^{-1}$  (Kulkarni et al. 2003). Furthermore, its study with low spatial resolution instruments is complicated by the presence of diffuse emission from the surrounding supernova remnant N49.

We started in 2003 a long-term monitoring program to study the time evolution of the spectral properties of SGR 1806–20 using the XMM-Newton X-ray satellite. Thanks to its imaging capability and large effective area we could obtain spectra of a much better quality than those available from previous satellites. The emission of the 27 December 2004 giant flare was also a fortunate occurrence, since we could observe how the source properties evolved in the two years leading to the flare and how they changed after this dramatic event (Mereghetti et al. 2005; Tiengo et al. 2005).

A similar observational campaign could not be carried out for SGR 1900+14. In fact this source is located in a sky region that, until recently, was not accessible to XMM-Newton observations due to technical constraints in the satellite pointing. Thus the first observation of SGR 1900+14 with this satellite could be obtained only in September 2005, during a long period of inactivity (the last bursts before the XMM-Newton observation were reported in November 2002, Hurley et al. 2002). SGR 1900+14 became active again in March 2006: bursts were observed by Swift (Palmer et al. 2006) and Konus-Wind (Golenetskii et al. 2006). We therefore requested a target of opportunity XMM-Newton observation, that was carried out on 1 April 2006.

## 2. Observations

We present the results obtained with the EPIC instrument, consisting of two MOS and one pn cameras (Turner et al. 2001; Strüder et al. 2001). In all the observations the pn was operated in Full Frame mode and the MOSs in Large Window mode (time resolution: 73.4 ms and 0.9 s respectively). Both the pn and the MOSs mounted the medium thickness filter. All the data were processed using version 6.5.0 of the *XMM-Newton Science Analysis System* and the most recent calibration files (last update on 2005 December 14). Response matrices and effective area files were generated ad-hoc with the SAS tasks *rmfgen* and *arfgen*; spectral fits were performed using the XSPEC v11.3 software (Arnaud 1996).

The first observation of SGR 1900+14 was divided in two parts, starting on 2005 Septem-

ber 20 01:44 UT and 22 01:36 UT, respectively. Since there was no evidence for variations in the flux and spectrum of the source from September 20 to 22, we added the two data sets and analyzed them together. After filtering for particle induced flares we obtained a net exposure time of 38.9 ks in the pn camera, and of 47.4 ks in the two MOSs.

The second observation started on 1 April 2006 and lasted  $\sim 22$  ks, yielding net exposure times of 12.7 ks in the pn camera and of 15.7 ks in the two MOSs.

The 0.8–10 keV image obtained with the pn camera in September 2005 is shown in Fig.1. SGR 1900+14 is the brightest source at the center of the field. Several other objects, detected here for the first time are visible. As expected for such a low Galactic latitude field, many of them can be associated with foreground stars based on their soft spectrum and positional coincidence with bright optical counterparts. A relatively bright spatially resolved source is also visible  $\sim 5'$  to the West of SGR 1900+14, but it is very likely unrelated to the SGR. Its spectrum is well described by an optically thin plasma emission model (MEKAL in XSPEC) with temperature  $kT = 7_{-2}^{+3}$  keV and a high absorption of  $N_{\text{H}} = (3.6_{-0.7}^{+1.0}) \times 10^{22} \text{ cm}^{-2}$ . This spectrum and the spatial extension of about one arcminute are consistent with emission from a cluster of galaxies at redshift  $z \sim 0.6$  and with a 2–10 keV luminosity of  $\sim 2 \times 10^{44} \text{ erg s}^{-1}$ . Its coordinates are R.A.= $19^{\text{h}} 06^{\text{m}} 53^{\text{s}}.7$ , Dec.= $+09^{\circ} 20' 47''$  (J2000).

### 3. Timing and spectral results

Except for the periodic pulsations, SGR 1900+14 did not show flux variability within the two observations, but it was about 15% brighter in April 2006, after the burst reactivation. We searched for the presence of bursts in both observations, by a careful analysis of light curves binned with different time resolution, but none could be found. With a standard folding analysis of the Solar system barycentered light curves, we measured a spin period of  $5.198346 \pm 0.000003 \text{ s}$  in September 2005 and  $5.19987 \pm 0.00007 \text{ s}$  in April 2006. In Figure 2 we show the background subtracted pulse profiles in three different energy ranges. The pulsed fractions (values reported in the corresponding figures) have been computed by fitting a sinusoid to the light curves. There is no evidence for changes in the pulsed fractions and light curve shapes between the two observations. The two period measurements correspond to a spin-down rate of  $(9.2 \pm 0.4) \times 10^{-11} \text{ s s}^{-1}$ .

We extracted spectra for SGR 1900+14 by selecting source counts with patterns 0–4 for the pn camera and 0–12 for the MOS cameras from circles of  $40''$  radius. The background spectra were extracted from composite regions located on the same chip as the source. The spectra were rebinned to have at least 30 counts in each bin and to oversample the

instrumental energy resolution by a factor three. Fits were performed in the energy range 0.8–12 keV, since the source is heavily absorbed and only few counts are detected at lower energies.

In Fig. 3 and 4 we show the spectrum obtained with the pn camera in the September 2005 observation, fitted with a power law and with a power law plus black body model, respectively. The latter clearly provides a better fit, as it can be seen from the residuals shown in the lower panels of the figures. Similar results were obtained using the spectra from the MOS. We therefore performed simultaneous fits of the spectra from the three cameras, obtaining photon index  $\Gamma=1.9\pm0.1$ , blackbody temperature  $kT=0.47\pm0.02$  keV, and absorption  $N_H = (2.12 \pm 0.08) \times 10^{22}$  cm<sup>-2</sup>. An acceptable fit could also be obtained with the sum of two blackbodies with temperatures of 0.53 and 1.9 keV (see Table 1).

The second observation gave entirely consistent spectral parameters, except for a statistically significant variation in the flux. The background subtracted count rates (0.8-10 keV) measured with the pn camera were  $0.615 \pm 0.004$  counts s<sup>-1</sup> in September 2005 and  $0.720 \pm 0.008$  counts s<sup>-1</sup> in April 2006. Indeed the April 2006 data are well described simply rescaling in normalization (by  $\sim 15\%$ ) the best fit spectra of the September 2005 observation.

For both observations we performed phase-resolved spectroscopy extracting the spectra for different selections of phase intervals. No significant variations with phase were detected, all the spectra being consistent with the model and parameters of the phase-averaged spectrum, simply rescaled in normalization.

No evidence for emission or absorption lines was found by inspecting the residuals from the best fit models. We computed upper limits on the lines equivalent widths as a function of the assumed line energy and width. This was done by adding Gaussian components to the model and computing the allowed range in their normalization. The most constraining results were obtained for the September 2005 observation. They are summarized in Figure 5, where the top panel refers to the phase averaged spectrum and the other ones to the spectra of the pulse maximum (phase from 0.25 to 0.75 of Fig. 2) and minimum.

#### 4. Discussion

Previous spectral studies of the persistent X-ray emission of SGR 1900+14, carried out with ASCA (Hurley et al. 1999), BeppoSAX (e.g., Woods et al. 1999a, Esposito et al. 2006 and references therein) and Chandra (Kouveliotou et al. 2001), showed that a blackbody plus power law model often provides a better fit than a single power law. The blackbody temperature was always of  $\sim 0.4$ - $0.5$  keV and the power law photon index  $\Gamma \sim 2$  (except for

the only BeppoSAX observation carried out before the 1999 giant flare, that had a harder spectrum with  $\Gamma=1.1$ ). The XMM-Newton best fit parameters are in agreement with these values, but the flux of  $\sim 4.8 \times 10^{-12}$  erg cm $^{-2}$  s $^{-1}$  measured in our September 2005 observation is the lowest ever detected from SGR 1900+14. A  $\sim 30\%$  decrease of the persistent emission, compared to the “historical” level of  $\sim 10^{-11}$  erg cm $^{-2}$  s $^{-1}$ , had already been noticed in the last BeppoSAX observation (Esposito et al. 2006), that was carried out in April 2002, six months earlier than the last bursts reported before the recent reactivation. This is illustrated in Fig. 6, where we have plotted the long term evolution of the pulse period, X-ray flux and bursting rate of SGR 1900+14.

The long term fading experienced by SGR 1900+14 in 2002-2005 might be related to the apparent decrease in the bursting activity in this period and can be compared to that of SGR 1627–41. SGR 1627–41 experienced a short period of bursting activity in June–July 1998 and, during the following  $\sim 2$  years, its 2-10 keV flux decreased with time as a power law  $F(t) \propto (t-t_0)^{-0.6}$ , with  $t_0$  indicating the time of the outburst (Mereghetti et al. 2006). As suggested by Kouveliotou et al. (2003), this behavior is likely due to the fact that, during outbursts, a substantial amount of energy is deposited in the deep crustal layers ( $\sim 500 - 600$  m in depth) due to shear dissipation and magnetic reconnection. Heat is then transported inwards (because the conductivity increases at larger densities) and later gradually transferred to the surface. Lyubarsky et al. (2002) computed the surface cooling evolution, in plane parallel approximation, by assuming a constant magnetic field perpendicular to the surface and by solving numerically the heat flow equation. They found that in a time scale of a few days the deep crustal layers are cooled by inward heat flow, and that 80% of the deposited energy is transferred to the core and re-radiated over longer timescales as surface X-ray emission. Quite independently on the details of the initial energy deposition, this model gives a cooling luminosity that scales in time as  $t^{-0.7}$ , in agreement to what has been observed for SGR 1627–41 (Mereghetti et al. 2006).

An alternative scenario to explain the “afterglows” following magnetars outbursts is that surface heating is caused by the currents flowing in an azimuthally twisted magnetosphere (Thompson et al. 2002; Gotthelf & Halpern 2005). The basic idea is that the toroidal component of the internal magnetic field stresses the crust, inducing a deformation and causing the external field to acquire an azimuthal component. In this case a current density in excess of the Goldreich-Julian current (which is expected for a simple dipolar field) is required to thread the magnetosphere. As the twist angle grows, the bursting activity is expected to increase and larger returning currents heat the star surface producing more thermal photons. By assuming a simple cylindrically symmetric and self-similar magnetosphere, Thompson et al. (2002) derived an upper limit for the luminosity of the returning currents,  $L_X^{rc} \simeq 10^{35} B_{14}^p \Delta\phi$  erg s $^{-1}$ , where  $\Delta\phi$  is the twist angle and  $B_{14}^p$  is the polar value of the magnetic

field in unit of  $10^{14}$  G. In this model the luminosity decay is dictated by the time evolution of the current (and that of the consequent, almost instantaneous surface heating), but no detailed computations have been performed so far.

The luminosity decay shown by SGR 1900+14 has been much smaller than that of SGR 1627–41, since the flux of the former source only faded by a factor  $\sim 2$  in three years. By fitting the observed decay with a power law gives  $F(t) \propto (t - t_0)^{-0.17}$ , where we have taken as  $t_0$  the time of the intermediate flare of 18 April 2001 (Feroci et al. 2003). The flatter slope may be an indication that a mechanism of the second kind (i.e. surface heating by returning currents) is at work. On the other hand, the one-dimensional model computed by Lyubarsky et al. (2002) assumed that the internal magnetic field is essentially radial. There is now increasing theoretical and observational evidence that strong poloidal and toroidal components can be present in the neutron star crustal magnetic field (see e.g. Geppert & Rheinhardt 2006 and references therein). This affects dramatically the heat transfer, that becomes strongly anisotropic. A strong magnetic field channels the heat flow along its field lines and, in the presence of large meridional components, can produce large inhomogeneities in the surface temperature distribution. Moreover, toroidal fields substantially limit the radial conductivity (heat blanketing) forcing energy to be transferred into narrow regions along the polar axis. Although no detailed computations are available, we may argue that, by assuming that the initial energy deposition per unit volume is the same, crustal fields with large poloidal and toroidal components might produce flatter power law luminosity decays, due to a combination of a smaller emitting surface area and of the lower efficiency of the radial conductivity in establishing a substantial thermal gradient between the core and the surface (the latter being proportional to the flux of heat outward).

We found no evidence for emission or absorption lines in the X-ray spectra. The upper limits obtained in the longer observation of September 2005 are the most constraining ever obtained for this source in the 1-10 keV energy range. An emission line at 6.4 keV was possibly detected with the PCA instrument on RXTE in August 1998 (Strohmayer & Ibrahim 2000). This line, visible only for the first 0.3 s of a particularly long and hard burst, had an equivalent width of  $\sim 400$  eV and was interpreted as Fe fluorescence from relatively cool material possibly ejected during the giant flare that occurred two days before its detection. Thus it is not surprising that we do not find evidence for the same feature in the spectrum of the persistent emission.

In models involving ultra-magnetized neutron stars, proton cyclotron features are expected to lie in the X-ray range, for surface magnetic fields strengths of  $\sim 10^{14} - 10^{15}$  G. Detailed calculations of the spectrum emerging from the atmosphere of a magnetar in quiescence have confirmed this basic expectation (Zane et al. 2001; Ho & Lai 2001). Model spectra

exhibit a strong absorption line at the proton cyclotron resonance,  $E_{c,p} \simeq 0.63z_G(B/10^{14} \text{ G})$  keV, where  $z_G$ , typically in the 0.70–0.85 range, is the gravitational red-shift at the neutron star surface. However, no evidence for persistent cyclotron features have been reported to date in SGRs, despite some features have been possibly detected during bursts (see e.g. Strohmayer & Ibrahim 2000; Ibrahim et al. 2003).

Indeed some reasons have also been proposed to explain the absence of cyclotron lines in magnetars, besides the obvious possibility that they lie outside the sampled energy range. First, it must be noticed that the atmospheric models available so far only account for a single temperature and a single value of magnetic field strength and inclination in the atmosphere, and no source of heating besides the standard core cooling is taken into account. Again, the lack of a standard atmosphere in active magnetars, and the fact that their magnetic field topology and surface temperature distribution are likely to be complex, makes the non detection of proton cyclotron features in the persistent emission not surprising.

Moreover, in the model discussed by Thompson et al. (2002), magnetars have highly twisted magnetospheres that can support current flows. These, in turn, can substantially distort the thermal emission from the neutron star surface. The presence of charged particles ( $e^-$  and ions) produces a large resonant scattering depth and the resonant frequency depends on the local value of the magnetic field. If the source flux at the cyclotron resonance does not exceed the luminosity of the returning currents, the distributions of both electrons and ions are spatially extended, in which case repeated scatterings could lead to the formation of a hard tail, typically observed below  $\sim 10$  keV, instead of a narrow line. Another implication of this model is that the twisted magnetospheres can act as a source of gamma rays, either through bremsstrahlung from a thin turbulent layer of the star’s surface heated to  $kT \sim 100$  keV by magnetospheric currents or through synchrotron emission from pairs produced at a height of  $\sim 100$  km above the neutron star (Thompson & Beloborodov 2005). Indeed a hard X-ray tail extending to 100 keV has been recently discovered in SGR 1900+14 with the INTEGRAL satellite Götz et al. (2006). A different explanation for the absence of lines involves vacuum polarization effects. It has been calculated that in strongly magnetized atmospheres this effect can significantly reduce the equivalent width of cyclotron lines, thus making difficult their detection (Ho & Lai 2003).

## 5. Conclusions

Thanks to the high sensitivity of the EPIC instrument on XMM-Newton we have obtained the first high quality spectra of the persistent X-ray emission from SGR 1900+14, setting tight limits on the presence of emission and absorption lines. In September 2005



the source was found at a luminosity level of  $1.3 \times 10^{35}$  erg s<sup>-1</sup> (for d=15 kpc), a factor two smaller than the typical value observed in the past, and in line with the trend of luminosity decrease already observed in the latest BeppoSAX observations performed in April 2002. The target of opportunity XMM-Newton observation of April 2006 showed that the decreasing luminosity trend in SGR 1900+14 has been interrupted by the recent onset of bursts emission. However, the moderate flux increase was not associated with significant changes in the X-ray spectral and timing properties, probably because the source is, up to now, only moderately active. Future observations with XMM-Newton will be essential to monitor the spectral and flux variations for this source, possibly in connection with its renewed bursting activity, as it has been successfully done for its twin source SGR 1806–20.

We thank N.Schartel and the staff of the XMM-Newton Science Operation Center for performing the target of opportunity observation. This work has been partially supported by the Italian Space Agency and INAF through contract ASI/INAF I/023/05/0 and by the MIUR under grant PRIN 2004-023189.

## REFERENCES

- Arnaud, K. A. 1996, in ASP Conf. Ser. 101: Astronomical Data Analysis Software and Systems V, ed. G. H. Jacoby & J. Barnes
- Cline, T. L., Desai, U. D., Pizzichini, G., et al. 1980, ApJ, 237, L1
- Duncan, R. C. & Thompson, C. 1992, ApJ, 392, L9
- Esposito, P., Mereghetti, S., Tiengo, A., et al. 2006, Submitted to A&A
- Feroci, M., Mereghetti, S., Woods, P., et al. 2003, ApJ, 596, 470
- Geppert, U. & Rheinhardt, M. 2006, accepted by A&A, [ArXiv: astro-ph/0606120]
- Golenetskii, S., Aptekar, R., Mazets, E., et al. 2006, GRB Circular Network, 4936
- Gotthelf, E. V. & Halpern, J. P. 2005, ApJ, 632, 1075
- Götz, D., Mereghetti, S., Tiengo, A., & Esposito, P. 2006, A&A, 449, L31
- Ho, W. C. G. & Lai, D. 2001, MNRAS, 327, 1081
- Ho, W. C. G. & Lai, D. 2003, MNRAS, 338, 233
- Hurley, K., Li, P., Kouveliotou, C., et al. 1999, ApJ, 510, L111

- Hurley, K., Mazets, E., Golenetskii, S., & Cline, T. 2002, GRB Coordinates Network, 1715
- Ibrahim, A. I., Swank, J. H., & Parke, W. 2003, *ApJ*, 584, L17
- Kouveliotou, C., Dieters, S., Strohmayer, T., et al. 1998, *Nature*, 393, 235
- Kouveliotou, C., Eichler, D., Woods, P. M., et al. 2003, *ApJ*, 596, L79
- Kouveliotou, C., Strohmayer, T., Hurley, K., et al. 1999, *ApJ*, 510, L115
- Kouveliotou, C., Tennant, A., Woods, P. M., et al. 2001, *ApJ*, 558, L47
- Kulkarni, S. R., Kaplan, D. L., Marshall, H. L., et al. 2003, *ApJ*, 585, 948
- Laros, J. G., Fenimore, E. E., Fikani, M. M., Klebesadel, R. W., & Barat, C. 1986, *Nature*, 322, 152
- Lyubarsky, Y., Eichler, D., & Thompson, C. 2002, *ApJ*, 580, L69
- Mazets, E. P., Golenetskii, S. V., & Guryan, Y. A. 1979, *Soviet Astronomy Letters*, 5, 343
- Mereghetti, S., Esposito, P., Tiengo, A., et al. 2006, *A&A*, 450, 759
- Mereghetti, S., Tiengo, A., Esposito, P., et al. 2005, *ApJ*, 628, 938
- Paczynski, B. 1992, *Acta Astronomica*, 42, 145
- Palmer, D., Sakamoto, T., Barthelmy, S., et al. 2006, *The Astronomer's Telegram*, 789
- Strohmayer, T. E. & Ibrahim, A. I. 2000, *ApJ*, 537, L111
- Strüder, L., Briel, U., Dennerl, K., et al. 2001, *A&A*, 365, L18
- Thompson, C. & Beloborodov, A. M. 2005, *ApJ*, 634, 565
- Thompson, C. & Duncan, R. C. 1995, *MNRAS*, 275, 255
- Thompson, C. & Duncan, R. C. 1996, *ApJ*, 473, 322
- Thompson, C., Lyutikov, M., & Kulkarni, S. R. 2002, *ApJ*, 574, 332
- Tiengo, A., Esposito, P., Mereghetti, S., et al. 2005, *A&A*, 440, L63
- Turner, M. J. L., Abbey, A., Arnaud, M., et al. 2001, *A&A*, 365, L27
- Woods, P. M., Kouveliotou, C., van Paradijs, J., Finger, M. H., & Thompson, C. 1999a, *ApJ*, 518, L103

Woods, P. M., Kouveliotou, C., van Paradijs, J., et al. 1999b, ApJ, 519, L139

Zane, S., Turolla, R., Stella, L., & Treves, A. 2001, ApJ, 560, 384

Table 1. Summary of the spectral results in the 0.8–12 keV energy range

Model <sup>a</sup>	Observation	$N_{\text{H}}$ ( $10^{22}$ cm <sup>-2</sup> )	$\Gamma$	$k_{\text{B}}T_1$ (keV)	$R_{\text{bb}1}^{\text{b}}$ (km)	$k_{\text{B}}T_2$ (keV)	$R_{\text{bb}2}^{\text{b}}$ (km)	Flux <sup>c</sup> ( $10^{-12}$ erg cm <sup>-2</sup> s <sup>-1</sup> )	$\chi_r^2$ (d.o.f.)
PL	A	$2.57 \pm 0.05$	$2.84 \pm 0.04$	...	...	...	...	$4.85 \pm 0.07$	1.65 (467)
...	B	$2.71 \pm 0.08$	$2.81 \pm 0.06$	...	...	...	...	$5.6 \pm 0.1$	1.21 (323)
BB+BB	A	$1.82 \pm 0.06$	...	$0.53^{+0.01}_{-0.02}$	$3.7^{+0.3}_{-0.2}$	$1.9 \pm 0.1$	$0.22 \pm 0.02$	$4.6 \pm 0.1$	1.32 (465)
...	B	$2.0^{+0.1}_{-0.2}$	...	$0.53^{+0.03}_{-0.02}$	$3.9 \pm 0.4$	$1.9^{+0.2}_{-0.1}$	$0.23^{+0.04}_{-0.03}$	$5.3 \pm 0.2$	1.04 (321)
PL+BB	A	$2.12 \pm 0.08$	$1.9 \pm 0.1$	$0.47 \pm 0.02$	$4.0^{+0.4}_{-0.3}$	...	...	$4.8 \pm 0.2$	1.24 (465)
...	B	$2.3^{+0.1}_{-0.2}$	$1.9 \pm 0.2$	$0.47 \pm 0.03$	$4.2 \pm 0.5$	...	...	$5.5 \pm 0.4$	1.00 (321)

<sup>a</sup>Errors are quoted at the 90% confidence level for a single parameter.

<sup>b</sup>Radius at infinity assuming a distance of 15 kpc.

<sup>c</sup>Flux in the 2–10 keV range, corrected for the absorption. The flux errors take into account the whole range of uncertainties in the spectral parameters.

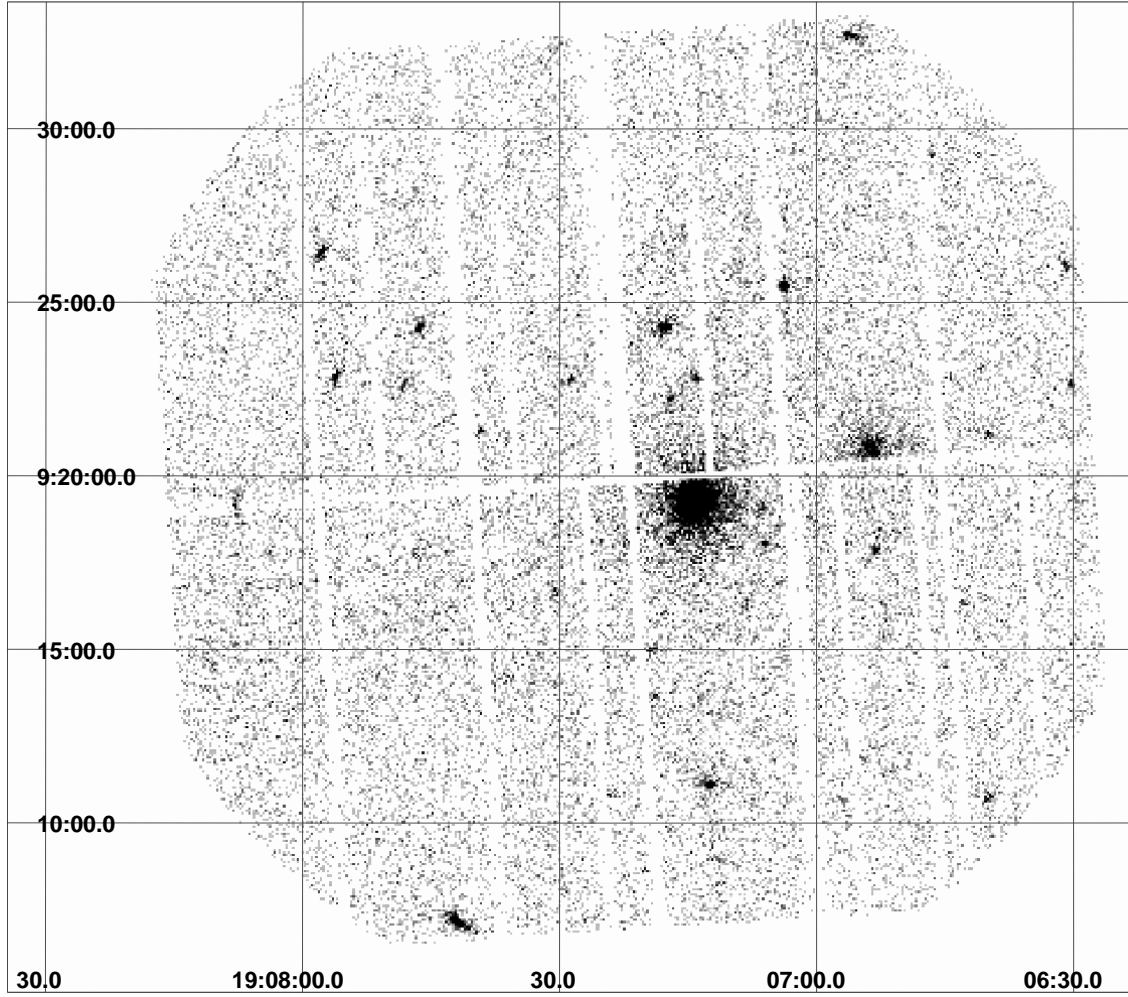


Fig. 1.— EPIC-pn image of the SGR 1900+14 field in the 0.8–10 keV energy range. North is to the top, East to the left.

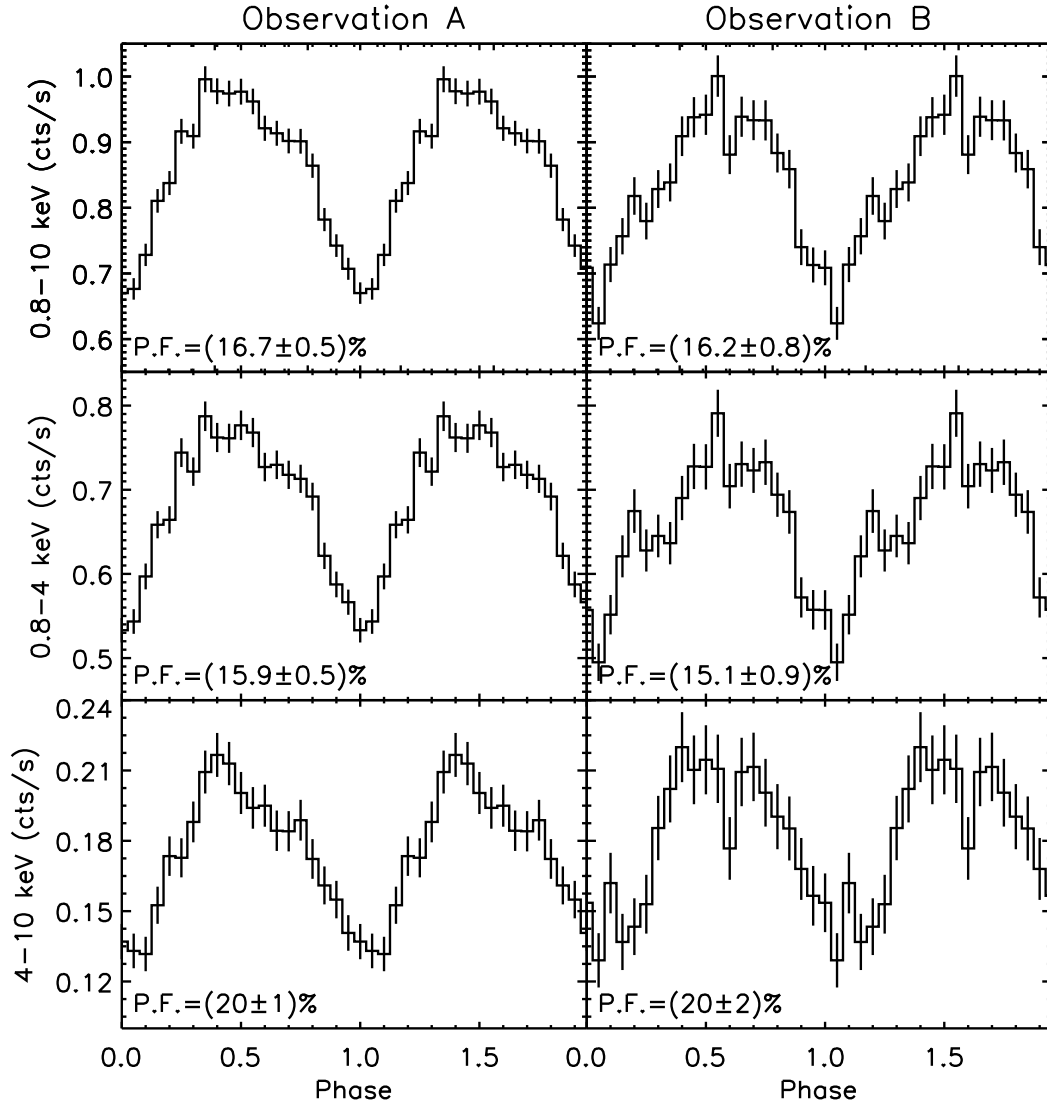


Fig. 2.— Folded light curves in the total (0.8-10 keV), soft (0.8-4 keV), and hard (4-10 keV) energy range for the two observations. The background has been subtracted. The corresponding pulsed fraction is indicated on each panel ( $1\sigma$  errors).

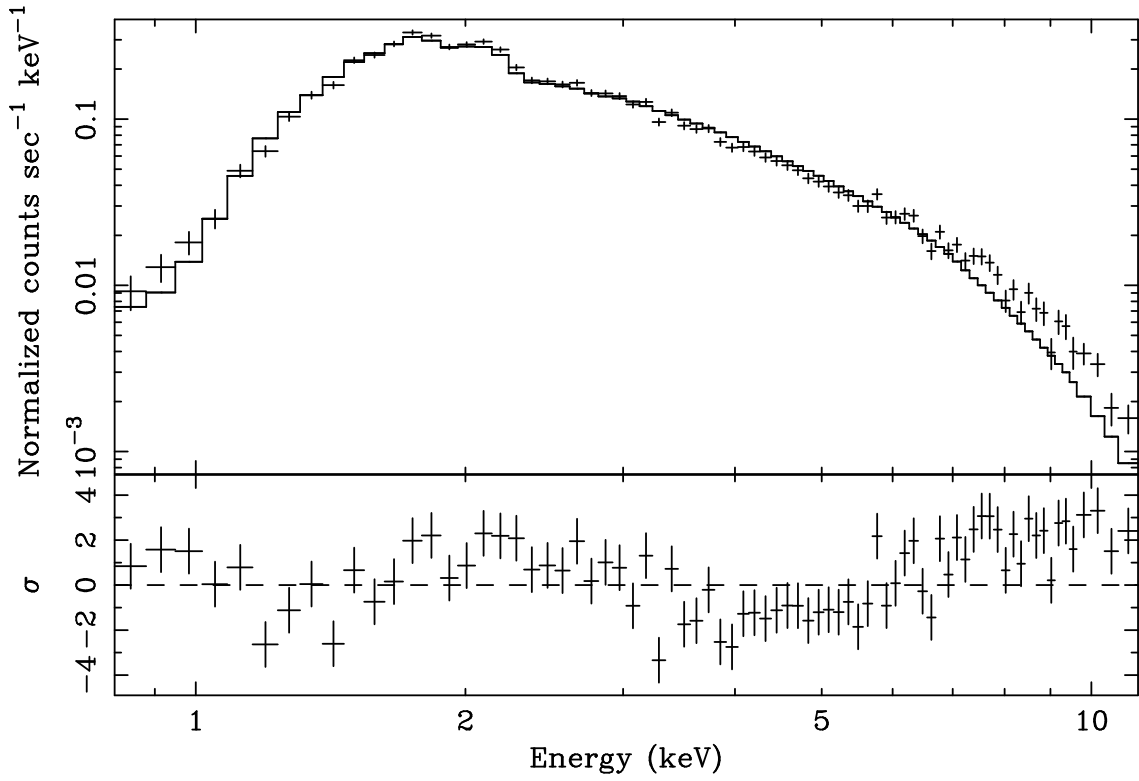


Fig. 3.— EPIC pn spectrum of SGR 1900+14 from the September 2005 observation. Top: data and best fit power law model. Bottom: residuals from the best fit model in units of standard deviations.

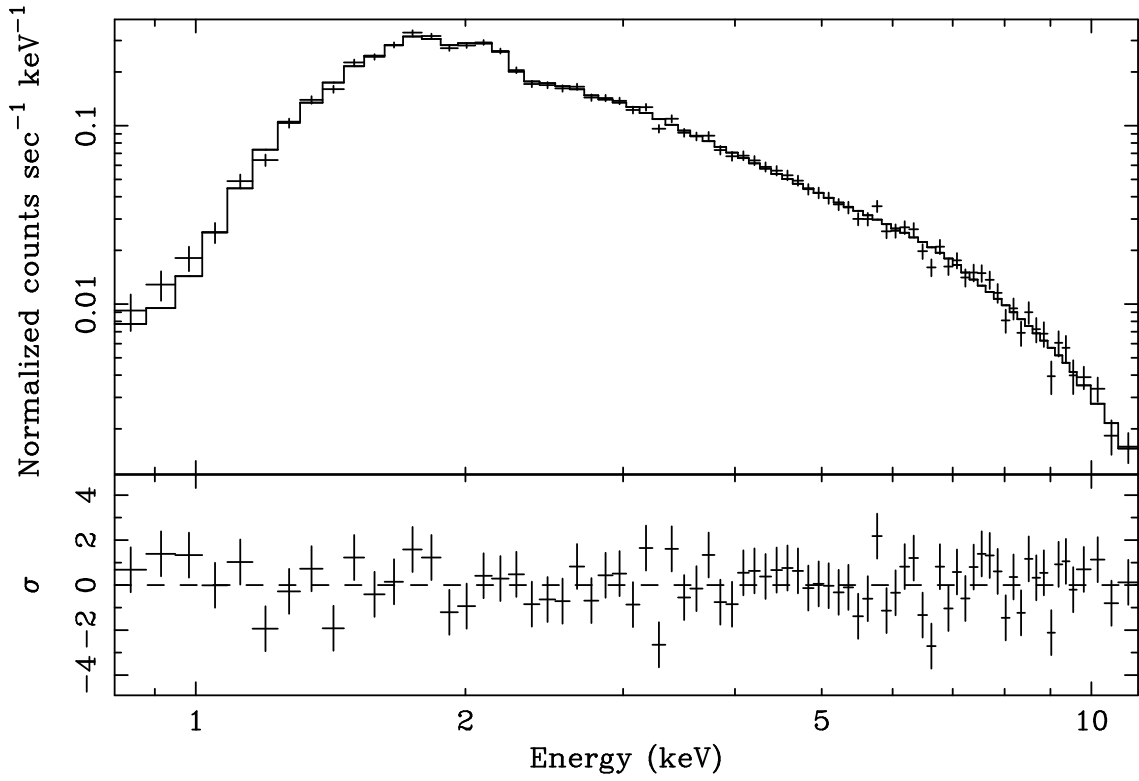


Fig. 4.— EPIC pn spectrum of SGR 1900+14 from the September 2005 observation. Top: data and best fit power law plus blackbody model. Bottom: residuals from the best fit model in units of standard deviations.



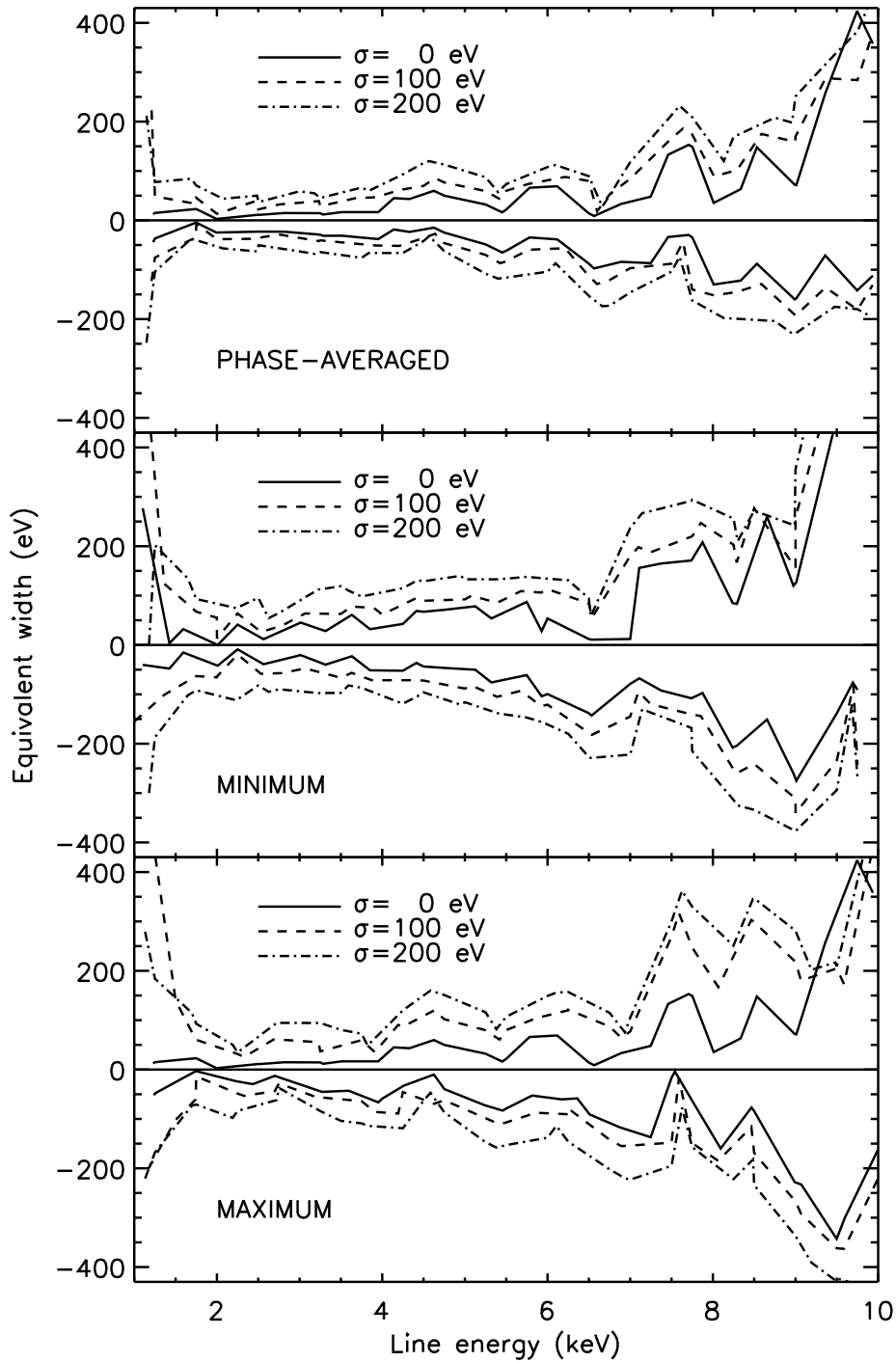


Fig. 5.— Upper limits (at  $3\sigma$ ) on spectral features in the 2005 pn data of SGR 1900+14 . The top panel refers to the phase-averaged spectrum and the two lower panels to the spectra at the pulse minimum and maximum.

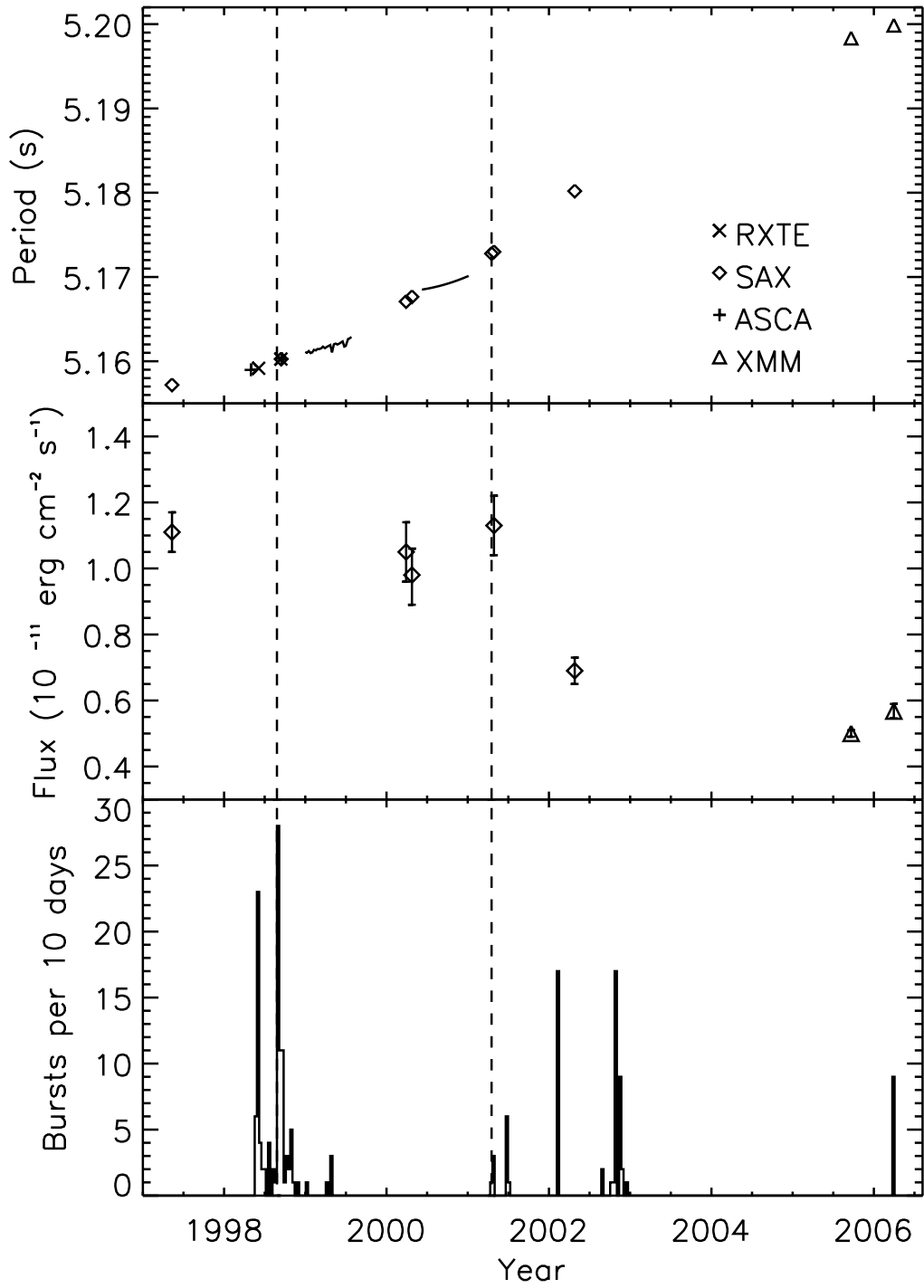


Fig. 6.— Long term evolution of the pulse period (top panel), X-ray flux (middle panel) and bursting rate observed with the IPN (bottom panel) of SGR 1900+14. The vertical dashed lines indicate the times of the 27 August 1998 giant flare and of the 18 April 2001 intermediate flare.